Journal of Advanced Marine Engineering and Technology, Vol. 49, No. 6, pp. 496~500, 2025
J. Advanced Marine Engineering and Technology (JAMET)
https://doi.org/10.5916/jamet.2025.49.6.496

ISSN 2234-7925 (Print)
ISSN 2765-4796 (Online)
Original Paper

Comparison of Corrosion Resistance Characteristics of Zn-Al-Mg Alloy Steel according to Cutting Methods

Beomsoo Kim[1] · Kyunghwang Lee[2] · Yeonwon Kim[3] · Jeonghyeon Yang[†]

(Received December 12, 2025 ; Revised December 19, 2025 ; Accepted December 24, 2025)

Abstract: The cutting method plays a critical role in determining the cut-edge quality and corrosion resistance of Zn–Al–Mg alloy-coated steel. This study systematically compared the corrosion behavior at cut edges produced by different cutting processes. Plasma cutting caused oxide formation and partial evaporation of the zinc layer, resulting in darkened cut surfaces and rapid initial red rust formation due to loss of sacrificial protection. Shear cutting induced localized mechanical deformation and coating damage, leading to progressive corrosion initiation at damaged regions. In contrast, waterjet cutting produced clean cut edges with minimal thermal and mechanical damage, thereby maintaining surface stability and delaying corrosion. Gradual color changes during exposure indicated the formation of corrosion products associated with oxidation and self-healing behavior. Overall corrosion resistance followed the order: waterjet > shear > laser > plasma cutting. These results demonstrate that minimizing thermal and mechanical damage at the cut edge is essential for preserving the sacrificial protective function of Zn–Al–Mg coatings. Accordingly, waterjet and precision shearing are recommended for marine and outdoor structural applications.

Keywords: Zn-Al-Mg alloy, Cutting method, Corrosion resistance, Self-healing

1. Introduction

Zn-Al-Mg alloy-coated steel is widely used in industrial applications requiring high corrosion resistance, such as marine structures. Under corrosive conditions, Zn is preferentially oxidized, and in the presence of chloride ions (Cl^-), a self-healing process occurs in which red rust is gradually covered by white rust due to the formation of simonkolleite **[1]**. This behavior serves as an effective protective barrier, particularly at cut edges.

Self-healing at cut edges generally requires a prolonged exposure period and is strongly influenced by environmental conditions. At these locations, the exposed base metal can act as a site for localized corrosion, which may directly reduce the durability and service life of the entire structure **[2]-[4]**.

In practical fabrication of steel structures, machining processes such as cutting, drilling, and welding are routinely applied to satisfy installation and assembly requirements. These processes may introduce thermal and mechanical damage, including partial coating evaporation, oxide formation, microstructural alteration, and exposure of the substrate. Therefore, for high-corrosion-resistant steels, the choice of cutting method appropriate to the material is an important factor governing cut-edge condition and subsequent corrosion performance. Common steel cutting processes include mechanical cutting, flame cutting, plasma cutting, and waterjet cutting, each exhibiting distinct characteristics. Mechanical cutting is performed without thermal input, thereby minimizing heat-affected zones, although localized micro-cracks may be introduced due to mechanical deformation. Flame cutting involves significant thermal input, which can induce oxidation and partial damage to the coating layer. Plasma cutting is characterized by high cutting speed and precision; however, the localized high-temperature exposure may result in coating degradation and surface damage at the cut edge. In contrast, waterjet cutting is a heatless process that effectively preserves the coating layer, making it particularly suitable for applications where maintaining coating integrity is critical.

Previous studies have reported on the evaluation of corrosion

† Corresponding Author (ORCID: http://orcid.org/0000-0002-6700-6234): Professor, Department of Mechanical System Engineering, Gyeongsang National University, 2 Tongyeonghaean-ro, Tongyeong, 53064, Korea, E-mail: jh.yagi@gnu.ac.kr, Tel: +82-55-772-9107
1 Professor, Department of Mechanical System Engineering, Gyeongsang National University, E-mail: kimbs@gnu.ac.kr, Tel: +82-55-772-9107
2 Ph. D., POSSOL INNOTECH, E-mail: ceo@possol.kr
3 Professor, Division of Marine Mechatronics, Mokpo National Maritime University, E-mail: k.yeonwon@mmu.ac.kr, Tel: +82-61-240-7237

This is an Open Access article distributed under the terms of the Creative Commons Attribution Non-Commercial License (http://creativecommons.org/licenses/by-nc/3.0), which permits unrestricted non-commercial use, distribution, and reproduction in any medium, provided the original work is properly cited.

Copyright ⓒ The Korean Society of Marine Engineering

resistance on the cut surface of Zn-Al-Mg layers, but there are very limited cases of analysis of corrosion resistance characteristics due to long-term exposure to the mechanism of interaction between the cutting method and the layer composition **[5][6]**.

Therefore, this study compared and analyzed the degree of layer damage and corrosion behavior at the cut surface of Zn-Al-Mg alloy steel by applying four cutting methods: shear, plasma, laser, and waterjet. Through this, the effect of processing method selection on securing corrosion resistance of Zn-Al-Mg alloy steel is identified, and the optimal processing strategy is presented according to thermal and mechanical damage at the cut surface.

2. Experimental Method

2.1 Specimens and Cutting Methods

In this study, Zn- 2.5% Al-3.0% Mg alloy steel was used. The substrate thickness was divided into four types, 1.6 mm, 2.0 mm, 3.0 mm, and 3.2 mm, and the coating weights were 60g/m²(M06) and 300 g/m²(M30). Each specimen was cut to a size of 100 × 150 mm, and no separate post-processing was performed. The cutting method was shear, plasma, laser, and waterjet cutting, which are cutting techniques widely used in industrial sites. The detailed sample specifications and the appearances of the cut edges produced by different cutting methods are summarized in **Table 1**. The cross-section was confirmed through SEM after cutting.

Table 1: Sample specifications and appearances of Zn–Al–Mg alloy-coated steel after cutting by different methods

Cutting method	Sample		Image
	Sample THK	Coating weight	
Plasma cutting (P)	1.6t(1) 2.0t(2) 3.0t(3) 3.2t(4)	M30 M30 M06 M30	
Laser cutting (L)	1.6t(1) 2.0t(2) 3.0t(3) 3.2t(4)	M30 M30 M06 M30	
Waterjet cutting (W)	1.6t(1) 2.0t(2) 3.0t(3) 3.2t(4)	M30 M30 M06 M30	
Shear cutting (S)	1.6t(1) 2.0t(2) 3.0t(3) 3.2t(4)	M30 M30 M06 M30	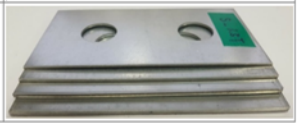

Table 2: Comparison of Salt Spray Test (SST) and Cyclic Corrosion Test (CCT) Conditions

Item	Salt Spray Test (SST)	Cyclic Corrosion Test (CCT)
Standard	ASTM B117	KS D ISO 14993
Test environment	Continuous salt spray	Repeated salt spray–dry–wet cycles
NaCl concentration	5 wt.%	5 wt.%
Spray temperature	35 °C	35 °C (spray stage)
Test cycle	Continuous exposure	1 cycle: spray (2 h) + drying (4 h) + wetting (2 h)
Drying stage	Not applied	60 °C for 4 h
Wetting stage	Not applied	50 °C for 2 h
Total test duration	65 days	165 cycles
Environmental variation	Single, constant condition	Multiple, cyclic conditions
Oxygen availability	Relatively limited	Enhanced during drying stage
Dominant corrosion mode	Mainly uniform corrosion	Accelerated localized corrosion
Simulation of outdoor exposure	Low	High
Sensitivity to cut-edge corrosion	Relatively low	Very high

2.2 Corrosion Resistance Evaluation and Analysis

The corrosion resistance was evaluated using a cyclic corrosion test and a salt spray test. The CCT was conducted according to KS D ISO 14993, with one cycle consisting of 35°C salt spray (2 h), 60°C drying (4 h), and 50°C wetting (2 h), for a total of 165 cycles. The SST was conducted according to ASTM B117, with a 5 wt.% NaCl solution sprayed at 35°C for 65 days. A comparative summary of the test conditions and environmental characteristics of the CCT and SST is provided in **Table 2**. The outdoor exposure test was conducted at a test site in Songdo, Incheon, under C4 conditions, with the cut-edge monitored for 6 to 24 months at a 30° south-facing slope.

3. Results and Discussion

3.1 SEM Image Analysis

Figure 1 shows FE-SEM images of the cut-edge cross sections after laser, waterjet, and shearing cutting. Plasma cutting was difficult to observe the cut surface due to damage of the coating layer and substrate. As the thickness of the substrate is thicker, the cutting energy is required. In the case of laser cutting, the coating layer burn out the surface due to the heat source. The shearing method, which is a mechanical cutting method, caused the crack of coating layer.

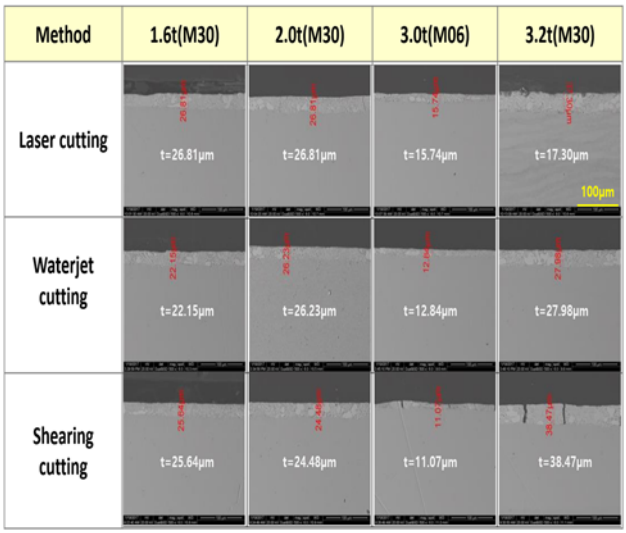

Figure 1: FE-SEM cross-sectional images of cut edges produced by different cutting methods

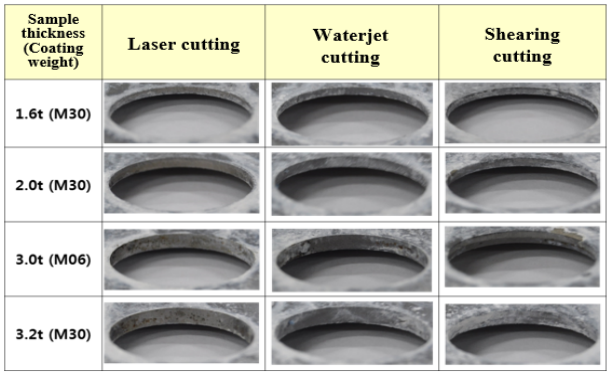

Figure 2: Cut-edge appearances after 165 cycles salt spray testing.

3.2 Results of Corrosion Resistance Evaluation

3.2.1 SST results

As shown in **Figure 2**, the SST evaluation after 165 cycles revealed no red rust formation at the cut edges, regardless of material thickness, coating weight, or cutting method.

3.2.2 CCT Results

On the other hand, as shown in **Figure 3**, significant red rust formation was observed around the hole-cut regions after 165 cycles of CCT under low coating weight conditions. In particular, the 1.6t samples exhibited red rust around the cut areas regardless of the cutting method. This apparent difference between the SST and CCT results can be explained by the fundamentally different exposure environments and corrosion mechanisms of the two tests. SST provides a continuous salt spray environment without a drying stage, resulting in limited oxygen replenishment and predominantly uniform corrosion, which facilitates the accumulation of protective corrosion products at the cut edge. In contrast, CCT involves repeated salt spray–dry–wet cycles, which enhance oxygen availability during the drying stage and repeatedly disrupt protective corrosion layers, thereby accelerating localized corrosion, particularly for thin substrates and low coating weights.

3.2.3 Outdoor Exposure Test Results

As a result of the 6 - month outdoor exposure test, a small amount of red rust occurred in the cut edge of 1.6t and 2.0t samples. As a result of the 19-month outdoor exposure test, the 1.6t sample showed a 90% or more coverage of red rust by white rust. The 2.0t sample did not decrease red rust but the white rust was relatively increased. The 3.2t samples showed a tendency of decreasing red rust of cut edge and hole after 19 months from 6 months after the start of the test. It is believed that this is due to the white corrosion products such as simonkolleite covering red rust.

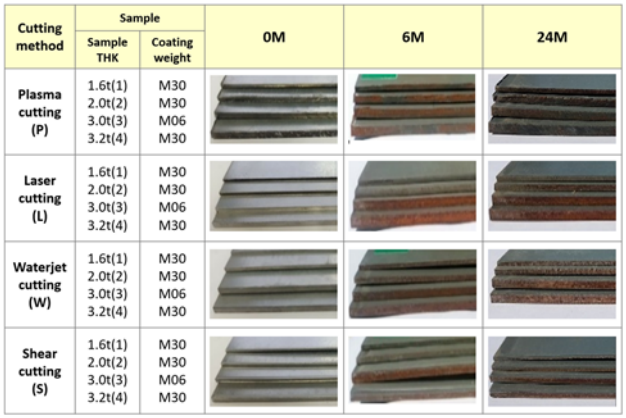

Figure 4: Cut-edge corrosion behavior during outdoor exposure testing

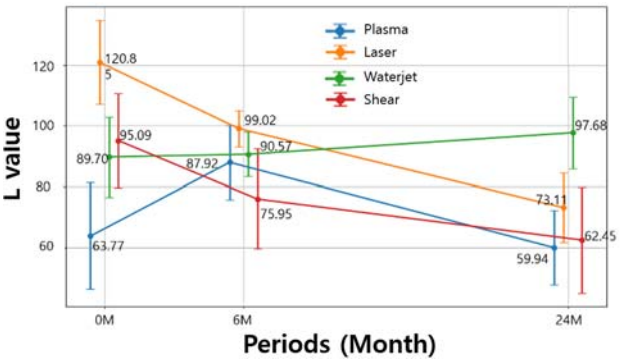

Figure 5: Changes in L value at the cut edge as a function of exposure time for different cutting methods

Plasma cutting is a process in which high temperatures of several thousand degrees Celsius are instantaneously applied to the cutting surface. During this process, the metal surface becomes molten or semi-molten and reacts rapidly with oxygen in the air. As a result, a dark red layer of Fe-oxide, as shown in **Figure 4**, is believed to have formed on the cutting surface. The measurement time points in **Figure 5** were selected based on representative stages of corrosion progression at the cut edge rather than at fixed time intervals.

Figure 5 shows the changes in the L value at the cut edge depending on the cutting method. In the case of plasma cutting specimens, the surface exhibited a blackened appearance immediately after cutting due to oxidation and thermal effects, resulting in a low L value. The formation of corrosion products led to a temporary increase in surface brightness, accompanied by a rise in the L value with increasing exposure time. However, as corrosion progressed further, the accumulation of red rust and corrosion products caused surface darkening, resulting in a subsequent decrease in the L value.

In specimens cut by shearing and laser cutting, a bright metallic surface was observed immediately after cutting, resulting in relatively high L values. As exposure time increased, corrosion products formed progressively at the cut edges, causing surface darkening and a gradual decrease in the L value.

3.3 Comparative Analysis of Corrosion Characteristics by Cutting Method

The initial corrosion rate and long-term stabilization behavior at the cut surface varied depending on the cutting method. These differences were mainly associated with the thermal effects introduced during the cutting process **[7]-[9]**. For waterjet cutting specimens, negligible heat input during cutting prevented the formation of a heat-affected zone, thereby minimizing oxidation and surface discoloration at the cut edge.

In addition, the coating layer and substrate experienced minimal microstructural damage, resulting in a stable initial surface condition. Consequently, the formation of corrosion products was suppressed, leading to only minor variations in surface lightness and a relatively constant L value over time.

3.3.1 Thermal Cutting Samples

The cut surfaces of thermally cut specimens (e.g., plasma cutting) exhibited rapid initial corrosion. At accelerated initial corrosion, the alloy components Mg, Al of the layer around the cut surface were transformed or volatilized by the high temperature, delaying the formation of the initial MgOH2 protective film **[10][11]**. This resulted in rapid initial corrosion, similar to that of conventional zinc **[12]**.

As time passed, the Mg component gradually dissolved from the intact layer around the cut surface and began to form a protective film, which resulted in a gradual decrease and stabilization of the corrosion rate at progressive stabilization.

3.3.2 Non-Thermal Cutting Samples

The cross-section of the specimens cut non-thermally (e.g., shearing) showed a gradual corrosion progression. Early Corrosion Inhibition: Since there was no thermal damage during the cutting process, the alloy composition of the layer was maintained, so the Mg component was effectively dissolved immediately after exposure, forming a rapid $MgOH_2$ protective film.

Continuous coating formation and healing: Slow corrosion progressed over time, but at the same time, the phenomenon of continuous protective film formation self-healing by Mg and Al components was observed, effectively controlling corrosion damage.

4. Conclusion

In this study, the effects of different cutting methods on cut-edge damage and corrosion behavior of Zn–Al–Mg alloy-coated steel were systematically investigated through microstructural observation and corrosion resistance evaluation. Based on the experimental results, the effects of cutting methods on cut-edge damage and corrosion behavior of Zn–Al–Mg alloy-coated steel were evaluated, and the main conclusions are summarized as follows.

1. The extent of coating layer damage and surface oxidation at the cut edge varied significantly depending on the cutting method, and this variation played a critical role in determining the long-term corrosion resistance of the material.
2. Thermal cutting processes, such as plasma and laser cutting, caused severe coating degradation due to evaporation of the Zn-based layer and oxide formation, resulting in rapid initial red rust formation and disruption of the sacrificial protection mechanism.
3. Non-thermal cutting methods exhibited improved cut-edge integrity; in particular, waterjet cutting preserved the coating layer most effectively and showed superior corrosion resistance, while shearing induced localized mechanical damage leading to gradual corrosion initiation.
4. Although the self-healing behavior of the Zn–Al–Mg

coating was observed regardless of the cutting method, higher coating preservation at the cut edge promoted faster and more stable corrosion protection. Consequently, the corrosion resistance ranking was determined as Waterjet > Shear > Laser > Plasma, indicating that waterjet and precision shearing are the most suitable cutting processes for offshore and outdoor structural applications.

Author Contributions

Conceptualization, B. Kim and J. Yang; Methodology, B. Kim; Validation, B. Kim and K. Lee; Investigation, Y. Kim and B. Kim; Resources, B. Kim; Data Curation, Y. Kim; Writing—Original Draft Preparation, B. Kim; Writing—Review & Editing, Y. Yang and Y. Kim; Visualization, Y. Kim; Supervision, K. Lee and J. Yang; Project Administration, J. Yang.

References

[1] H. Schürz, M. Fleischanderl, G. Mori, and H. Luckeneder, "Corrosion behaviour of Zn–Al–Mg coated steel sheet in sodium chloride-containing environment," Corrosion Science, vol. 51, no. 10, pp. 2355-2363, 2009.

[2] J. W. Lee, S. J. Kim, and M. S. Oh, "Influence of alloy content on microstructure and corrosion resistance of Zn-based alloy coated steel product," Korean Journal of Metals and Materials, vol. 58, no. 3, pp. 169–174, 2020.

[3] S. Wang, N. Xie, X. Ma, S. Chen, H. Liu, R. Ma, A. Du, X. Zhao, Y. Fan, "Study on the self-healing behavior and corrosion mechanism of hot-dip Zn–6Al–3Mg alloy coatings in corrosive environments," Surfaces and Interfaces, vol. 74, 107714, 2025.

[4] R. Krieg, M. Rohwerder, S. Evers, B. Schuhmacher, J. Schauer-Pass, "Cathodic self-healing at cut-edges: The effect of Zn2+ and Mg2+ ions," Corrosion Science, vol. 65, pp. 119-127, 2012.

[5] M. S. Oh, S. H. Kim, J. S. Kim, J. W. Lee, J. H. Shon, and Y. S. Jin, "Surface and cut-edge corrosion behavior of Zn-Mg-Al alloy-coated steel sheets as a function of the alloy coating microstructure," Metals and Materials International, vol. 22, pp. 26-33, 2016.

[6] J. W. Lee, B. R. Park, S. Y. Oh, D. W. Yun, J. K. Hwang, M. S. Oh, "Mechanistic study on the cut-edge corrosion behaviors of Zn-Al-Mg alloy coated steel sheets in chloride containing environments," Corrosion Science, vol. 160, 108170, 2019.

[7] K. Lipiäinen, A. Ahola, E. Virolainen, A. Hirvi, T. Björk, "Fatigue strength of hot-dip galvanized S960 cut edges and longitudinal welds," Journal of Constructional Steel Research, vol. 189, 107083, 2022.

[8] S. Sheikholeslami, G. Williams, H. N. McMurray, L. Gommans, S. Morrison, S. Ngo, D. E. Williams, and W. Gao, "Cut-edge corrosion behavior assessment of newly developed environmental-friendly coating systems using the Scanning Vibrating Electrode Technique (SVET)," Corrosion Science, vol. 192, 109813, 2021.

[9] A. G. Marques, J. Izquierdo, R. M. Souto, and A.M. Simões, "SECM imaging of the cut edge corrosion of galvanized steel as a function of pH," Electrochimica Acta, vol. 153, pp. 238-245, 2015.

[10] T. Prosek, D. Persson, J. Stoulil, and D. Thierry, "Composition of corrosion products formed on Zn–Mg, Zn–Al and Zn–Al–Mg coatings in model atmospheric conditions," Corrosion Science, vol. 86, pp. 231-238, 2014.

[11] S. H. Kim, S. Y. Jin, J. H. Yang, J. H. Yang, M. H. Lee, and Y. S. Yun, "Self-healing phenomenon at the cut edge of Zn–Al–Mg alloy coated steel in chloride environments," Coatings, vol. 14, no. 4, 485, 2024.

[12] T. E. Graedel, "Corrosion mechanisms for zinc exposed to the atmosphere," Journal of The Electrochemical Society, vol. 136, no. 4, p. 193C, 1989.